Theor Chem Acc (2001) 107:8–14
DOI 10.1007/s002140100291

Theoretical
Chemistry Accounts

Regular article

Molecular dynamics, density functional and second-order Møller–Plesset theory study of the structure and conformation of acetylcholine in vacuo and in solution

T. Marino[1], **N. Russo**[1], **E. Tocci**[2], **M. Toscano**[1]

[1]Dipartimento di Chimica and Centro di Calcolo ad Alte Prestazioni per Elaborazioni Parallele e Distribuite-Centro d'Eccellenza MURST, Università della Calabria, 87030 Arcavacata di Rende, Italy
[2]IRMERC-CNR-Università della Calabria, 87030 Arcavacata di Rende, Italy

Received: 4 April 2001 / Accepted: 5 July 2001 / Published online: 30 October 2001

Abstract. Molecular mechanics minimizations based on the CVFF force field and molecular dynamics simulation for a time of 2.5 ns were performed to examine the conformational behaviour and the molecular motion of acetylcholine in vacuo and in aqueous solution. Five low-lying conformations, namely the TT, TG, GG, G*G and GT, were obtained from molecular mechanics computations with the GT structure as the absolute minimum. Molecular dynamics trajectories in vacuo and in water show that only four (GT, GG, G*G and TG) and three (TG, TT and GT) conformations are present in the simulation time, respectively. Density functional B3LYP and second-order Møller–Plesset (MP2) methods were then used to study all the five lowest-lying conformers of acetylcholine neurotransmitter in vacuo and in water by the polarizable continuum model approach. The B3LYP and MP2 computations show that in the gas phase all minima lie in a narrow range of energy with the G*G conformer as the most stable one. The relative minima GG, GT, TG and TT are located at 1.1 (3.3), 1.8 (4.2), 2.1 (4.5) and 4.3 (7.3) kcal/mol above the absolute one at the B3LYP (MP2) level. The preferred conformation in water is the TG. Solvation reduces the relative energy differences between the five minima in both computations.

Key words: Acetylcholine – Density functional theory – Second-order Møller–Plesset – Molecular dynamics – Solvent effects

Correspondence to: N. Russo
e-mail: nrusso@unical.it

1 Introduction

The biological action of acetylcholine (ACh^+) in the transmission processes of nerve impulses is carried on all the synapsis of the autonomic central nervous system. The knowledge of its conformational behaviour is a topic of central interest in biological structure–activity relationships relevant to molecular pharmacology because the structure of cholinergic receptors has not been well established yet [1, 2]. The activity of ACh^+ on both nicotinic and muscarinic sites was related to its conformational flexibility [3–6]. In fact, this small molecule governs different important functions, including the binding to receptors of the postsynaptic membrane and its degradation by acetylcholinesterase (AChase), two processes highly dependent upon overall molecular conformations. For this reason, the structure and the conformational properties of ACh^+ have been the subject of many theoretical and experimental studies in the gas, liquid and solid states [4, 7–30].

The different conformations of ACh^+ derive from the rotation of the four internal torsional angles (Scheme 1). Because two of these angles (τ_0 and τ_3) were found to be near the trans value (180°) in most of the previous experimental [7–9] and theoretical [4, 11, 16, 22, 25–30] investigations, the conformational flexibility of ACh^+ can be ascribed to the remaining C–C–O–C (τ_1) and N^+–C–C–O (τ_2) dihedral angles (Scheme 1). Starting from an early X-ray study of Canepa et al. [5] and Sorum [31], several techniques, including NMR [10, 12–15, 19, 21], X-ray [5, 7, 8, 31–38], electron diffraction [39] and Raman spectroscopy [20], were used for the determination of the ACh^+ structure. From a theoretical point of view, many computational methods (i.e. ab initio, semiempirical, empirical and molecular dynamics, MD, methods) were employed [4, 9, 11, 16–18, 22–30, 40, 41] in order to ascertain its conformational behaviour. However, notwithstanding this impressive number of works, many problems remain to be clarified and

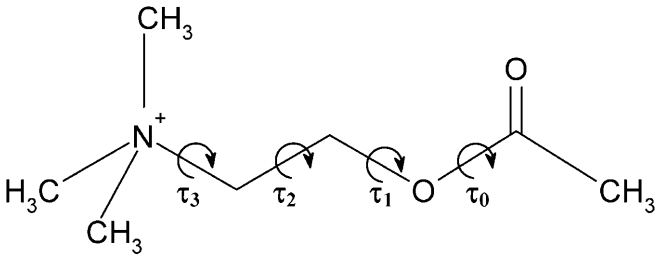

Scheme 1. The different conformations of acetylcholine from the rotation of the four internal torsional angle

the lack of high-level first principles computations to be filled. To our knowledge, only HF/STO-3G [25, 26, 30] and 4-21G [22] calculations have been done on ACh^+. A selection of the ACh^+ conformations previously proposed using experimental and theoretical methods is reported in Table 1. As is evident ACh^+ can exhibit different conformations even in the crystalline state. This is a further indication of its high flexibility as well as the possible existence of different conformations very close in energy. Thus, the study of environmental effects on the high mobility of this relatively small molecular system assumes great importance. With regard to this problem, our study was performed in the gas phase and in presence of solvent with the aim of predicting the optimum conformation to engage the receptor in aqueous media. MD simulations were used to explore the conformational behaviour of ACh^+ as a function of time.

Table 1. Conformation of acetylcholine (ACh^+) from selected previous theoretical and experimental studies

Conformers	τ_1	τ_2	Method	Reference
TG	193	85	X-ray	[7]
GG	79	78	X-ray	[7]
GG	83	89	X-ray	[8]
TG	180	78	X-ray	[8]
TG	165	80	X-ray	[8]
GG	105	75	X-ray	[8]
TG	172	90	X-ray	[8]
GG	118	85	X-ray	[8]
TT	180	180	EPF	[9]
GG	−76.0	179.8	EPF	[9]
TG	178.0	−73.6	EPF	[9]
GG	−75.4	−72.2	EPF	[9]
TT	180	180	NMR	[10]
TG	180	60	PCILO	[11]
G*G	120	−80	PCILO	[11]
G	–	–	NMR	[12–15]
TG	179	274	EPF	[16]
TT	177	172	EPF	[16]
G*G	−102	60	EPF	[17]
TG*	160	100	EPF	[17]
GT	−75.0	150	INDO	[18]
TG	180	60	NMR	[19]
TG	160	300	Raman	[20]
GG	260	280	Raman	[20]
TG	169	78	MNDO	[4]
TT	–	–	NMR	[21]
TG	171	65	HF/4-21G	[22]
GG*	70	225	EPF	[23]
TT	180	180	HF/FSGO	[24]
TG	180	60	HF/STO-3G	[25]
TG	150	60	HF/STO-3G	[26]
TG	180	80	EHT	[27]
G*G	100	300	INDO	[28]
TG	179.9	75.8	MD	[29]
TG	180.0	60.0	HF/STO-3G	[30]

2 Computational details

All quantum mechanical calculations were carried out using the GAUSSIAN 98 [42] code. Geometry optimizations, without imposing any symmetry constraints, were performed using the hybrid Becke [43] and Lee, Yang and Parr [44] (B3LYP) exchange–correlation functional and the second-order Møller–Plesset (MP2) method. In both cases the basis set used was 6-31G(d, p). Harmonic vibrational frequencies were computed at B3LYP and Hartree–Fock (HF) levels. The polarizable continuum model (PCM) [45–47] was used in order to evaluate the bulk solvent effects. The geometries in solution were fully optimized starting from those obtained in the gas phase, with the same methods and basis set.

MD and molecular mechanics (MM) simulations in vacuo and in water were performed using the CVFF [48] force field as implemented in the Insight/Discover codes [49]. Solvation was accomplished by placing the ACh^+ molecule in an equilibrated three-dimensional grid solvent in a simulation box of 22-Å side with 252 molecules of water. MD trajectories were produced in both media at constant number of particles, constant temperature and constant volume (NVT ensemble) and the temperature was controlled through direct bath-temperature coupling in order to obtain a broader sampling of conformational space. MD simulations were performed at 300 K for 2.5 ns with a time step of 1 fs. The positions and velocities of all the atoms of the structures were saved each 0.5 ps in a history file. The simulation time was chosen to be long enough to overcome the approach to the equilibrium (when trajectories move from arbitrarily assigned initial conditions) to span the equilibration state regions.

The quenching procedure [50–52] was applied after 300 ps of simulation and snapshots were taken every 250 ps. A total of 27 and 38 frames were selected from water and in vacuo dynamics, respectively. Subsequently, these structures were optimized with the conjugate-gradient algorithm until 0.01-kcal/Å maximum derivative.

The quantum mechanical computations in solvent, performed in this work, can be used as verification of the CVFF force field that was never previously tested in solution for ACh^+.

3 Results and discussion

As a first step, MM computations were used to build up the potential-energy surface of ACh^+ in vacuo around the τ_1 and τ_2 dihedral angles. For a fixed value (180°) of τ_1, τ_2 was varied in steps of 10°, starting from 0.0°, to 360.0°. The τ_1 torsion was then incremented by 10° and the process was repeated until a complete round angle was scanned. A total of 1369 frames were optimized, giving rise to a potential-energy map (Fig. 1) very similar to those previously drawn employing different force fields [4, 9, 16, 17].

As shown in Table 2, five minima lying in a very narrow range of energy, less than 1.5 kcal/mol, and corresponding to the TT, TG, GG, G*G and GT conformations (Fig. 2) were obtained. The GT conformation is the absolute minimum.

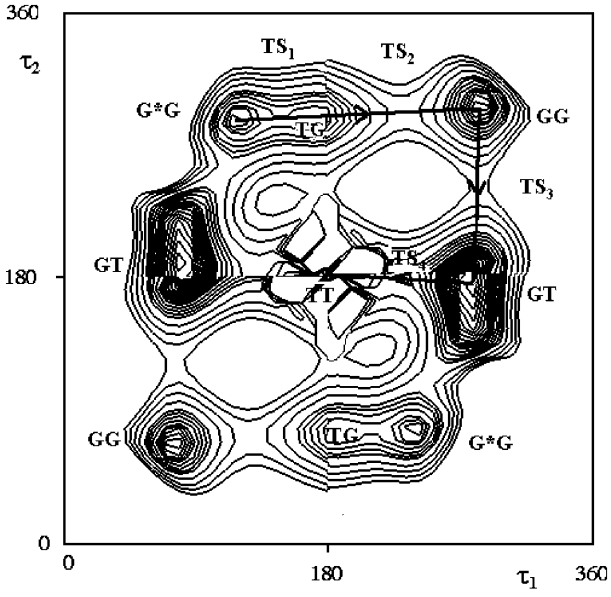

Fig. 1. Conformational energy map around the main τ_1 and τ_2 torsional angles of acetylcholine (ACh^+) by molecular mechanics. The energy contours are determined by a 10° resolution scan. Starting from the absolute minimum (102.2 kcal/mol) the first 12 isoenergetic contour lines are separated by 0.1 kcal/mol, the next five lines by 0.2 kcal/mol and the remaining five lines by 0.5 kcal/mol

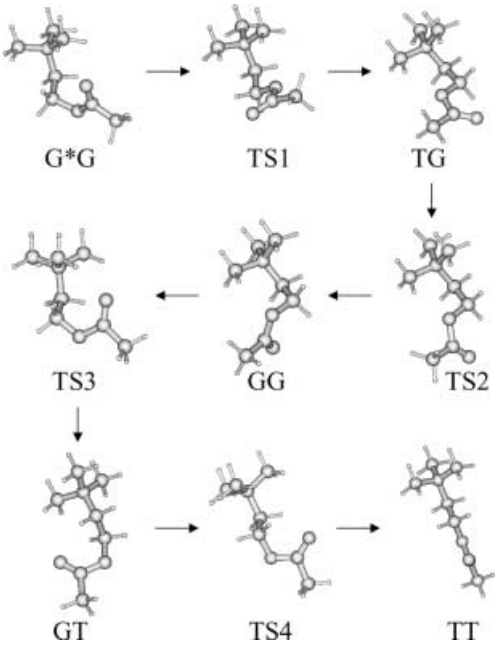

Fig. 2. Picture of minima and transition states (*TS*) along the energetic path of ACh^+

Table 2. Relative energies (ΔE in kcal/mol) of the ACh^+ conformers from conformational map in Fig. 1. The torsional angles are in degrees and the distances are in angstroms

Conformers	τ_1	τ_2	ΔE	—C=O—N^+
GT	80.1	170.1	0.0	4.33
GG	−74.2	60.2	0.7	4.11
G*G	119.9	−70.1	0.8	3.97
TT	−170.1	179.9	0.9	5.36
TG	−170.1	70.1	1.16	5.05

Table 3. Relative energies (ΔE in kcal/mol) of the ACh^+ sconformers in vacuo and in water. The torsional angles are in degrees and the distances are in angstroms

Conformers	τ_1	τ_2	ΔE	—C=O—N^+
Molecular dynamics in vacuo				
GT	80.5	172.6	0.0	4.37
GG	74.5	65.2	0.6	4.27
G*G	117.7	72.2	0.8	3.93
TG	−172.4	72.9	1.14	5.08
Molecular dynamics in water				
TG	174.07	71.7	0.0	5.28
TT	158.8	169.3	8.2	5.40
GT	88.92	171.6	19.2	4.61

3.1 MD in vacuo

The results of the MD simulation show that the most populated conformations in vacuo (GT, GG, G*G and TG in Fig. 2) fall, as in the case of the MM computations, in a very narrow range of energy (0.0–1.14 kcal/mol) (Table 3), while the TT conformation does not appear during the simulation time irrespective of the starting conformation chosen.

The distance between the carbonyl oxygen and the nitrogen of the trimethylammonium group, the cationic head, which is a parameter crucial to biological activity because it is important in the molecular interaction with AChase [6], has, in our MM calculations, values of about 4–5 Å, with a minimum in the G*G conformation (3.93 Å) (Table 3).

From the MD simulation in vacuo, in the minimum-energy conformer, the τ_2 torsional angle value determines a trans disposition of the particular molecular portion. This result is in disagreement with a series of experimental studies [7, 8, 19, 20] in which it was observed that the τ_2 dihedral is often in the gauche conformation. The reason for which the gauche conformation should be favoured was justified by invoking that "ACh^+ can be considered a member of a class of 1,2-disubstituted ethanes in which the increased stability of the gauche conformation is the norm. The stabilization of the gauche conformation was thought to involve electrostatic interactions and/or hydrogen bonding between the partially negative ester oxygen and a hydrogen atom of one of the three methyl groups of the cationic head" [4, 53–57]. The close proximity of the quaternary nitrogen to the ester oxygen should explain the increased stability of the gauche conformation. Because no significant interaction between the ester oxygen and any portion of the cationic head was previously observed or confirmed by our computations, the motivation for the increased stability of the gauche relative to the trans conformation remains unclear. On the other hand, there should be little probability of hydrogen-like bonds es-

pecially if the hydrogen atoms of the methyl group are involved. In addition, our results are referred to the in vacuo situation in which no intermolecular forces can act, so comparison with the crystallographic data is hard. However, the narrow range of energy that separates the conformations can justify the fact that in a particular environment the intermolecular forces and the hydrogen bond can stabilize one of these conformations.

The behaviour of the dihedrals τ_1 and τ_2 during the simulation time is shown in Fig. 3. For τ_1, after 1-ns simulation time, a fast alternation between gauche and trans values can be observed. The τ_2 values indicate that the trans conformation is prevalent, although the gauche ones are sometime reached.

3.2 MD in water

The conformational behaviour in water is quite different with respect to that in the gas phase. The quenching procedure allows many conformations to be extracted subjected to a further minimization (see Computation details). From this procedure it is found that the only conformers present in the MD trajectory are TG, TT and GT (Table 3). The absolute minimum is the TG conformation, followed by the TT and GT ones at 8.2 and 19.2 kcal/mol, respectively. The interaction with water causes a strong destabilization of the G*G and GG structures, which go up in energy to more than 20 kcal/mol above the absolute minimum. Furthermore, the energy differences between TG, TT and GT increase sensibly with respect to that obtained in vacuo. Intermolecular hydrogen bonds between the carboxylic moiety of ACh^+ and water molecules were found in all three minima.

The distances between the carbonyl oxygen and the cationic head are longer than those in vacuo (4.6–5.4 Å), with a minimum in the GT conformation (4.61 Å). This indicates that in water ACh^+ prefers more extended conformations.

The variations of the dihedrals τ_1 and τ_2 as a function of simulation time in water are shown in Fig. 4. For τ_1, a high variability is evident: values characteristic of the trans and gauche conformations occur alternatively every few picosecond during the entire simulation time (2.5 ns). For τ_2, the situation is very different. In fact, after the first 500 ps of the simulation, the trans conformation appears to be the preferred one, while the gauche one is present only occasionally. In any case, the global minimum has a value of τ_2 torsion that determines the gauche position of the molecular portion involved. Similar results were obtained previously from Monte Carlo hydration calculations [40] and from in NMR studies [12–15, 19]. In all the conformations selected different hydrogen bonds between the oxygen of the C=O group and water were found. The distances varied from a minimum of 1.70 Å, in the GT form, to a maximum of 2.01 Å, in the TG one. As in the Monte Carlo study [40], the cationic head appears to be more solvated than the carbonyl ester group (carboxylic moiety), showing that the hydrophilic character of ACh^+ is mainly related to this molecular region.

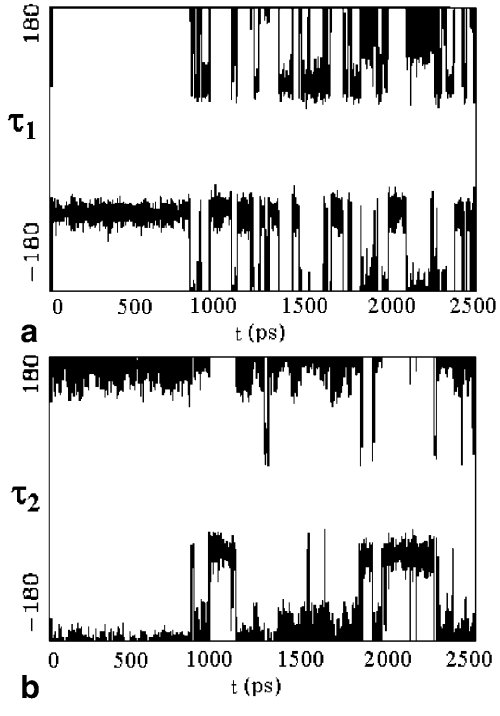

Fig. 3. Evolution of **a** τ_1 and **b** τ_2 torsional angles as function of time in the gas phase by molecular dynamics

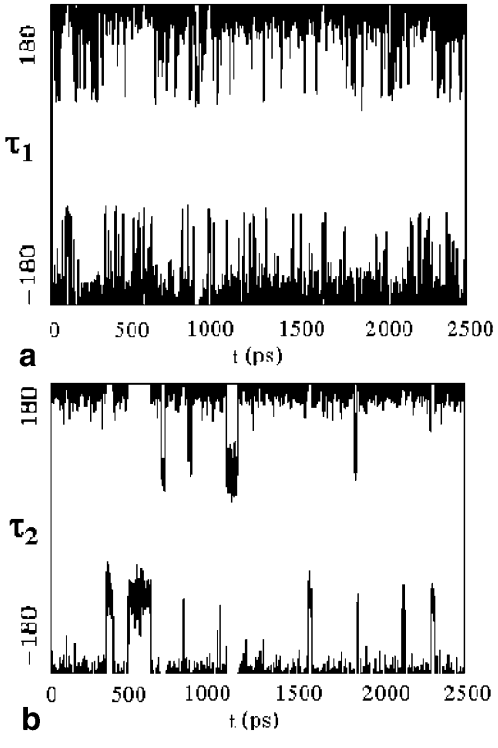

Fig. 4. Evolution of **a** τ_1 and **b** τ_2 torsional angles as function of time in water by molecular dynamics

3.3 First principles computations

Starting from the molecular geometries obtained from the MM optimizations, the five conformers of ACh^+ were fully reoptimized at the HF, MP2 and B3LYP levels using the double-zeta 6-31G(d, p) basis set. The results are collected in Table 4. At the HF level, the GG, GT and TG minima are almost degenerate in energy and the G*G and TT relative minima lie at 2.7 and 2.3 kcal/mol, respectively, above the absolute one (GG). Comparison with a previous HF/4-21G study [22] is possible only for the TG and TT conformers. In this latter investigation the TG form is more stable than the TT one, which lies 3.0 kcal/mol above the global minimum. The reduction of the energy gap between the TT and TG forms, in our HF computations, is clearly due to the different expansion of the basis set. The introduction of the correlation effects via the MP2 procedure modifies sensibly the HF results. In fact, the absolute minimum conformation becomes the G*G structure, followed by the GG form at 3.3 kcal/mol. The GT and TG conformers have about the same energy but their energy separation (ΔE) is now up to 4 kcal/mol. The less stable minimum appears to be the TT one, with a ΔE of 7.3 kcal/mol. The B3LYP results are in qualitative agreement with the MP2 ones, but the relative energy values differ. The most stable conformation is the same (G*G) as in the MP2/6-31G(d, p) computations and the lowest-lying relative minimum is again the GG form ($\Delta E = 1.1$ kcal/mol). The GT and TG conformers have almost the same energy, with a ΔE lower than in the MP2/6-31G(d, p) case. Finally, the more extended conformation (TT) appears to be the least stable, having a ΔE of 4.3 kcal/mol. The structures obtained with these two methods are similar as can be noted from the values of the torsional angles and from the $-C=O-N^+$ distances (Table 4), so the difference in the relative energy values can be ascribed to the different treatment of correlation contribution in the two methods.

Bulk water effects were introduced via the PCM method [45–47], which allows the geometries to be optimized in the solvent environment. Because of the size of the ACh^+ molecule, full optimization in solvent was done only at the HF and B3LYP levels and single-point energy computations were performed at the MP2 level using the HF-optimized geometrical parameters. The results are reported in Table 5. No sensible change is observed between the in vacuo and in the solvent geometrical structures. The only noticeable variation concerns the torsional angle τ_2 in the TG conformation, which increases from 62.4° (60.6°) in vacuo to 83.5° (76.1°) in solvent at the HF (B3LYP) levels (Tables 4, 5). The absence of relevant structural modifications is furthermore underlined by the constancy of the $-C=O-N^+$ distance values reported in Tables 4 and 5.

As a general trend, all the methods employed indicate that the five minima lie in an energy range that is smaller than that existing in the gas phase. HF prefers the TG conformation over the GG, TT, GT and G*G ones. Upon the introduction of the MP2 corrections, the absolute minimum conformation remains the same, with the GG conformer degenerate in energy. ΔE of the other minima have about the same values defining an energy range of about 2 kcal/mol. Similar indication comes from the B3LYP computations. Again the TG and GG conformers are degenerate and are preferred over the other ones by a few kilocalories per mole. It is worth noting that in contrast to the in vacuo computations, the extended conformation (TT) is not the least stable one in water. These trends can be explained by

Table 4. Gas-phase relative energies (ΔE in kcal/mol) at 0 K for the minima and transition states on the potential-energy surface of ACh^+. The torsional angles are in degrees and the distances are in angstroms

Conformers	τ_1	τ_2	ΔE	$-C=O-N^+$
HF/6-31G(d, p)				
G*G	111.8	75.8	2.7	3.547
GG	76.7	66.8	0.0	4.073
GT	78.9	158.5	0.5	3.834
TG	171.2	58.9	0.6	4.857
TT	180.0	180.0	2.3	5.115
MP2/6-31G(d, p)				
G*G	112.3	76.6	0.0	3.568
GG	78.6	67.1	3.3	4.183
GT	79.8	155.8	4.5	3.817
TG	170.8	62.4	4.2	4.968
TT	179.9	179.9	7.3	5.112
B3LYP/6-31G(d, p)				
G*G	114.5	71.5	0.0	3.590
GG	79.6	66.3	1.1	4.235
GT	78.5	153.7	2.1	3.764
TG	163.6	60.6	1.8	5.046
TT	177.9	179.1	4.3	5.127
TS_1	158.5	69.5	3.8	4.636
TS_2	125.0	61.0	1.9	4.995
TS_3	70.8	127.3	5.7	3.325
TS_4	81.2	178.4	7.0	4.228

Table 5. Relative stabilities in solvent (ΔE in kcal/mol) and free solvation energies (ΔG_{solv} in kcal/mol) for the conformers of ACh^+. The torsional angles are in degrees and the distances are in angstroms

Conformers	τ_1	τ_2	ΔE	ΔG_{solv}	$-C=O-N^+$
HF/6-31G(d, p) SCRF/PCM					
G*G	119.6	77.7	2.9	−58.5	3.850
GG	85.4	68.6	0.9	−60.7	4.444
GT	84.5	157.9	2.2	−59.8	4.027
TG	176.8	83.5	0.0	−62.9	4.976
TT	179.8	178.8	1.3	−62.6	5.173
MP2/6-31G(d, p) SCRF/PCM//HF/6-31G(d, p) SCRF/PCM					
G*G	119.6	77.7	1.7	−58.5	3.850
GG	85.4	68.6	0.1	−60.7	4.444
GT	84.5	157.9	1.8	−59.8	4.027
TG	176.8	83.5	0.0	−62.9	4.976
TT	179.8	178.8	1.5	−62.6	5.173
B3LYP/6-31G(d, p) SCRF/PCM					
G*G	109.1	78.5	1.6	−56.6	3.582
GG	86.8	67.4	0.4	−59.3	4.481
GT	79.9	152.9	2.8	−57.4	3.895
TG	174.5	76.1	0.0	−61.2	5.029
TT	179.9	179.4	1.8	−61.1	5.188

the different solvation energies (Table 5). Looking at the conformational energy map (Fig. 1) it is possible to understand why the relative energies can change dependent on the method employed or on the environmental conditions. The three minima lie in a unique energy channel that, for the same value of τ_2 (around 60° or 300°), includes a wide conformational space in the τ_1 direction. The minima are separated by maxima of about 4 and 6 kcal/mol, indicating that the mobility around τ_1 is high and relatively small energy perturbations can allow the transition between the various conformers. The characterization of these maxima as transition states (TS) was performed at the B3LYP level. The geometries of the TS are depicted in Fig. 2 and the relative energies are reported in Table 4. The TS, which separates the G*G and TG minima (TS_1), lies 3.8 kcal/mol above the absolute minimum (G*G) and is characterized by a τ_1 value of 158.5°. As expected the τ_2 value remains essentially the same. The transition between the TG and GG conformers occurs via TS_2, with an interconversion barrier of only 0.1 kcal/mol. The geometry of TS_2 has a τ_1 value of 125.0°, which is intermediate between the values characterizing the TG and GG conformations. The energy channel for the GG→GT transition is along the τ_2 angle as is evident from the conformational energy map in Fig. 1. The TS for this conformational transition (TS_3) has a τ_2 value of 127.3° and the barrier is 4.6 kcal/mol. The barrier for the GT→TT transition is due to the presence of another TS (TS_4), which has a value of 4.9 kcal/mol. The entire B3LYP energy path is reported in Fig. 5. As shown, the TG→GG conformational change occurs practically without an energy barrier, while the other three transitions are slightly more difficult. These results clearly show the high conformational flexibility of ACh^+, which can be related to the versatility of this neurotransmitter to act as a substrate for muscarinic, nicotinic and AChase sites.

Finally, the comparison between the first principles and the MD results in solution shows that in both cases conformer TG of ACh^+ is the most stable one and that the order of the other two relative minima obtained by the MD simulation is the same than that found at the MP2 and B3LYP levels.

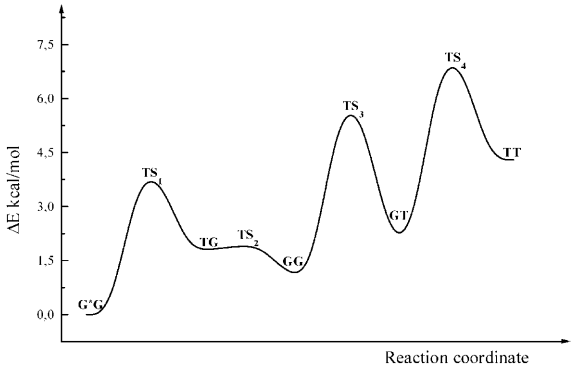

Fig. 5. B3LYP energetic path of ACh^+

4 Conclusions

We explored the conformational behaviour of the ACh^+ neurotransmitter at high levels of theory. The results showed that

- The five minima located in the conformational energy map lie in a narrow range of energy. The location of the TSs allows the high flexibility of ACh^+ around its main torsional angles to be explained.
- Bulk solvent effects do not change drastically the energy range in which all five minima fall in the gas phase. In water, all the first-principles-based methods employed agree in predicting the TG conformer as the absolute minimum, followed by the GG one as the lowest relative minimum.
- MD simulation for 2.5 ns indicates the presence in water solution of only the TG, TT and GT conformations.

Acknowledgements. This work was supported by the Università della Calabria, MURST-MEMOBIOMAR and CINECA.

References

1. Hucho F, Tsetlin VI, Machold J (1996) Eur J Biochem 239: 539
2. Furois-Corbin S, Pullman A (1989) Biochim Biophys Acta 984: 339
3. Berthier G, Savinelli R, Pullman A (2000) Theor Chem Acc 104: 78, and references therein
4. Egan MA, Zoeller RW (1993) J Org Chem 58: 1719
5. Canepa FG, Pauling P, Sorum H (1966) Nature 210: 907
6. Wilson IB (1957) Neurology 41
7. Svinnig T, Sorum H (1975) Acta Crystallogr Sect B 31: 1581
8. Jagner S, Jensen B (1977) Acta Crystallogr Sect B 33: 2757
9. Liquori AM, Damiani A, De Caen JL (1968) J Mol Biol 33: 445
10. Cushley RJ, Mautner HG (1970) Tetrahedron 26: 2151
11. Pullman B, Courriere P, Coubeils JL (1971) Mol Pharmacol 7: 397
12. Partington P, Feeney S, Burgen ASV (1972) Mol Pharmacol 8: 269
13. Mautner HG, Dexter DD (1972) Nature New Biol 238: 87
14. Terui Y, Veyama M, Satoh S (1974) Tetrahedron 30: 1465
15. Lichtenberg D, Kroon P, Chan S (1974) J Am Chem Soc 96: 5934
16. Weintraub AH, Hopfinger HJ (1974) Jerusalem Symp Quantum Chem Biochem 7: 131
17. Beveridge DL, Radna RJ (1974) Jerusalem Symp Quantum Chem Biochem 7: 153
18. Gelin BR, Karplus MJ (1975) J Am Chem Soc 97: 6996
19. Cassidei L, Sciacovelli O (1981) J Am Chem Soc 103: 933
20. Wilson JK, Derreumaux P, Vergoten G, Peticolas WL (1989) J Phys Chem 93: 1351
21. Behr JP, Lehn JM (1972) Biochem Biophys Res Commun 49: 1573
22. Klimkowski VJ, Schafer L, Scarsdale JN, Alsenoy CU (1984) J Mol Struct (THEOCHEM) 109: 311
23. Froimowitz M, Gans PJ (1972) J Am Chem Soc 94: 8020
24. Genson DW, Christoffersen RE (1973) J Am Chem Soc 95: 362
25. Port GNJ, Pullman A (1973) J Am Chem Soc 95: 4059
26. Pullman A, Port GNJ (1973) J Theor Chem 32: 77
27. Kier LB (1967) Mol Pharmacol 3: 487
28. Radna RJ, Beveridge DL, Bender AL (1973) J Am Chem Soc 95: 3831
29. Edvardsen O, Dahl SG (1991) J Neural Transm 83: 157
30. Pullman B, Berthod H, Gresh NCR (1975) Acad Sci t280: 1741
31. Sorum H (1959) Acta Chem Scand 13: 345

32. Shefter E, Kennard O (1966) Science 153: 1389
33. Herdklotz JK, Saaa RL (1970) Biochem Biophys Res Commun 40: 583
34. Mahajan V, Sass RL (1974) J Cryst Mol Struct 4: 15
35. Marzotto A, Graziani R, Bombieri G, Forsellini E (1974) J Cryst Mol Struct 4: 253
36. Sax M, Rodrigues M, Blank G, Wood MK, Pletcher J (1976) Acta Crystallogr Sect B 32: 1953
37. Datta N, Mondal P, Pauling P (1980) Acta Crystallogr Sect B 36: 906
38. Jensen B (1982) Acta Crystallogr Sect B 38: 1185
39. Jack JJ, Hercules DM (1971) Anal Chem 43: 729
40. Margheritis C, Corongiu G (1988) J Comput Chem 9: 1
41. Belcastro M, Marino T, Mineva T, Russo N, Sicilia E, Toscano M (1996) In: Seminario JM (ed) Recent development and applications of modern density functional theory, vol 4. Elsevier, Amsterdam, p 743
42. Frisch MJ, Trucks GW, Schlegel HB, Scuseria GE, Robb MA, Cheeseman JR, Zakrzewski VG, Montgomery JA, Stratmann RE Jr, Burant JC, Dapprich S, Millam JM, Daniels AD, Kudin KN, Strain MC, Farkas O, Tomasi J, Barone V, Cossi M, Cammi R, Mennucci B, Pomelli C, Adamo C, Clifford S, Ochterski J, Petersson GA, Ayala PY, Cui Q, Morokuma K, Malick DK, Rabuck AD, Raghavachari K, Foresman JB, Cioslowski J, Ortiz JV, Baboul AG, Stefanov BB, Liu G, Liashenko A, Piskorz P, Komaromi I, Gomperts R, Martin RL, Fox DJ, Keith T, Al-Laham MA, Peng CY, Nanayakkara A, Gonzalez C, Challacombe M, Gill PMW, Johnson B, Chen W, Wong MW, Andres JL, Gonzalez C, Head-Gordon M, Replogle ES, Pople JA (1998) Gaussian 98. Gaussian, Pittsburgh, Pa
43. Becke AD (1993) J Chem Phys 98: 5648
44. Lee C, Yang W, Parr RG (1988) Phys Rev B 37: 785
45. Barone V, Cossi M, Tomasi J (1998) J Comput Chem 19: 404
46. Barone V, Cossi M (1998) J Phys Chem A 102: 1995
47. Tomasi J, Persico M (1994) Chem Rev 94: 2027
48. Dauber-Osguthorpe P, Roberts VA, Osguthorpe DJ, Wolff J, Genest M, Hagler AT (1988) Proteins Struct Funct Genet 4: 31
49. Biosym Technologies Inc Insight/Discover codes. Biosym Technologies Inc, San Diego, Calif, USA
50. Fantucci P, Mattioli E, Villa AM, Villa L (1992) J Comput-Aided Mol Des 6: 315
51. Villa A, Fantucci P, Marino T, Russo N (1995) J Comput-Aided Mol Des 9: 425
52. Tocci E, Marino T, Toscano M, Russo N (1997) Gazzetta 127: 795
53. Wolfe S, Rauk A, Tel LM, Csizmadia I (1971) J Chem Soc B 136
54. Wolfe S (1972) Acc Chem Res 5: 102
55. Beveridge DL, Radna RL (1971) J Am Chem Soc 93: 3759
56. Donahue J (1968) Structural chemistry and molecular biology. Freeman, San Francisco
57. Craven BM, Hite G (1972) Acta Crystallogr Sect B 29: 1132